

SPREP

Chapter 5 **Fiji Islands**

5.1 Climate Summary

5.1.1 Current Climate

- Annual and half-year maximum and minimum temperatures have been increasing at both Suva and Nadi Airport since 1942 with trends significant at the 5% level in all cases except Nadi Airport November–April maximum temperature. Minimum air temperature trends are greater than maximum air temperature trends.
- The annual numbers of Cool Days and Cool Nights have decreased and Warm Nights have increased at both sites. Warm Days have increased at Suva. These temperature trends are consistent with global warming.
- Annual, half-year and extreme daily rainfall trends show little change at Suva and Nadi Airport since 1942.
- Tropical cyclones affect Fiji mainly between November and April, and occasionally in October and May during El Niño years. An average of 28 cyclones per decade developed within or crossed Fiji's Exclusive Economic Zone (EEZ) between the 1969/70 and 2010/11 seasons. Twenty-five out of 78 (32%) tropical cyclones between the 1981/82 and 2010/11 seasons

became severe events (Category 3 or stronger) in Fiji's EEZ. Available data are not suitable for assessing long-term trends.

- Wind-waves around Fiji are typically not large, with wave heights around 1.3 m year-round. Seasonally, waves are influenced by the trade winds, location of the South Pacific Convergence Zone (SPCZ), southern storms, and cyclones, and display little variability on interannual time scales with the El Niño–Southern Oscillation (ENSO) and Southern Annular Mode (SAM) (see Box 1). Available data are not suitable for assessing long-term trends.

5.1.2 Climate Projections

For the period to 2100, the latest global climate model (GCM) projections and climate science findings indicate:

- El Niño and La Niña events will continue to occur in the future (*very high confidence*), but there is little consensus on whether these events will change in intensity or frequency;

- Annual mean temperatures and extremely high daily temperatures will continue to rise (*very high confidence*);
- There is a range in model projections in mean rainfall, with the model average indicating little change in annual rainfall but an increase in the November–April season (*low confidence*), with more extreme rain events (*high confidence*);
- The proportion of time in drought is projected to decrease slightly (*low confidence*);
- Ocean acidification is expected to continue (*very high confidence*);
- The risk of coral bleaching will increase in the future (*very high confidence*);
- Sea level will continue to rise (*very high confidence*); and
- Wave height is projected to decrease across the Fiji area in the wet season, with a possible small increase in dry season wave heights (*low confidence*).

5.2 Data Availability

There are currently 21 climate stations (single observation at 9 am), 14 synoptic stations (multiple daily observations) and 40 rainfall-only stations (excluding the National Hydrology Network) operational in Fiji's meteorological network. There are at least six stations or multi-station composites with records available before 1900.

The complete historical rainfall and air temperature records for Laucala Bay (Suva) and Nadi Airport from 1942 have been used in this report. Suva and Nadi Airport are located on the south-eastern and western sides of Viti Levu respectively. Both records are homogeneous and more than 95% complete. Additional information on historical climate trends in the Fiji region can be found in the Pacific Climate Change Data Portal www.bom.gov.au/climate/pccsp/.

Wind-wave data from buoys are particularly sparse in the Pacific region, with very short records. Model and reanalysis data are therefore required to detail the wind-wave climate of the region. Reanalysis surface wind data have been used to drive a wave model over the period 1979–2009 to generate a hindcast of the historical wind-wave climate.

5.3 Seasonal Cycles

Information on temperature and rainfall seasonal cycles can be found in Australian Bureau of Meteorology and CSIRO (2011).

5.3.1 Wind-driven Waves

Surface wind-wave driven processes can impact on many aspects of Pacific Island coastal environments, including: coastal flooding during storm wave events; coastal erosion, both during episodic storm events and due to long-term changes in integrated wave climate; characterisation of reef morphology and marine habitat/species distribution; flushing and circulation of lagoons; and potential shipping and renewable wave energy solutions. The surface offshore wind wave climate can be described by characteristic wave heights, lengths (wave period) and directions.

The wind-wave climate of Fiji shows significant spatial variability along the coast due to the size of the main island and the prevailing winds.

At Suva, on the south-east coast of Viti Levu, waves are predominantly directed from the south-southeast throughout the year, with only small variation in wave heights. During June–September mean waves are largest (seasonal mean height around

1.7 m), consisting of trade wind generated waves from the south-east, and southerly and south-westerly swell propagated from storm events in the Southern Ocean (Figure 5.1). During December–March mean waves reach a minimum (seasonal mean height around 1.3 m), directed from the south-east, with increasing wave period as the season progresses (Table 5.1). Waves larger than 2.9 m (99th percentile) at Suva are predominantly directed from the south-east, with some large waves from other directions observed, particularly in March, likely associated with cyclones. The height of a 1-in-50 year wave event at Suva is calculated to be 7.8 m.

Near Nadi on the west coast of Viti Levu, waves are generally small and directed from the west due to being sheltered from the prevailing trade winds. Wave height does not vary significantly throughout the year (Figure 5.2), while period is slightly longer in the shoulder seasons between the wet and dry seasons. During December–March, waves at Nadi are more north-westerly. These waves consist predominantly of small magnitude swell waves with some influence from cyclones. During June–September, the observed waves are small and directed from the west with long periods (Table 5.1). There is a

small fraction of locally generated wind waves usually from the south-east resulting from the trade winds, or the north during the wet season. Waves larger than 1.0 m (99th percentile) occur mostly in December–March from the north-west, and are due to tropical cyclones, e.g. Cyclone Gavin on 8 March 1997. The height of a 1-in-50 year wave event at Nadi is calculated to be 4.3 m.

No suitable dataset is available to assess long-term historical trends in the Fiji wave climate. However, interannual variability may be assessed in the hindcast record. The wind-wave climate displays some interannual variability at Nadi and Suva, varying somewhat with the El Niño–Southern Oscillation (ENSO) and the Southern Annular Mode (SAM). During El Niño years at Nadi, there is an anticlockwise rotation of the direction from which the waves are travelling with respect to La Niña years. At Suva, wave power is greater and direction slightly more easterly during December–March in El Niño years, associated with suppression of trade winds due to the South Pacific Convergence Zone (SPCZ) in La Niña years. When the SAM index is negative, a slight southerly rotation in waves in June–September at Suva is due to enhanced mid-latitude storms in the Southern Ocean.

Table 5.1: Mean wave height, period and direction from which the waves are travelling around Fiji in December–March and June–September. Observation (hindcast) and climate model simulation mean values are given for Fiji with the 5–95th percentile range (in brackets). Historical model simulation values are given for comparison with projections (see Section 5.5.6 and Table 5.7). A compass relating number of degrees to cardinal points (direction) is shown.

		Hindcast Reference Data (1979–2009), Suva	Hindcast Reference Data (1979–2009), Nadi	Climate Model Simulations (1986–2005) – Fiji
Wave Height (metres)	December–March	1.3 (0.8–2.1)	0.4 (0.2–0.8)	1.6 (1.2–1.9)
	June–September	1.7 (1.0–2.5)	0.5 (0.2–0.7)	1.8 (1.4–2.2)
Wave Period (seconds)	December–March	9.1 (6.8–11.8)	10.2 (5.9–13.4)	8.3 (7.3–9.3)
	June–September	9.6 (7.2–12.4)	10.4 (5.7–14.2)	8.2 (7.2–9.3)
Wave Direction (degrees clockwise from North)	December–March	140 (90–190)	290 (260–340)	120 (80–150)
	June–September	160 (120–210)	270 (190–330)	140 (120–160)



Mean annual cycle of wave height and mean wave direction (hindcast)
Suva, Fiji

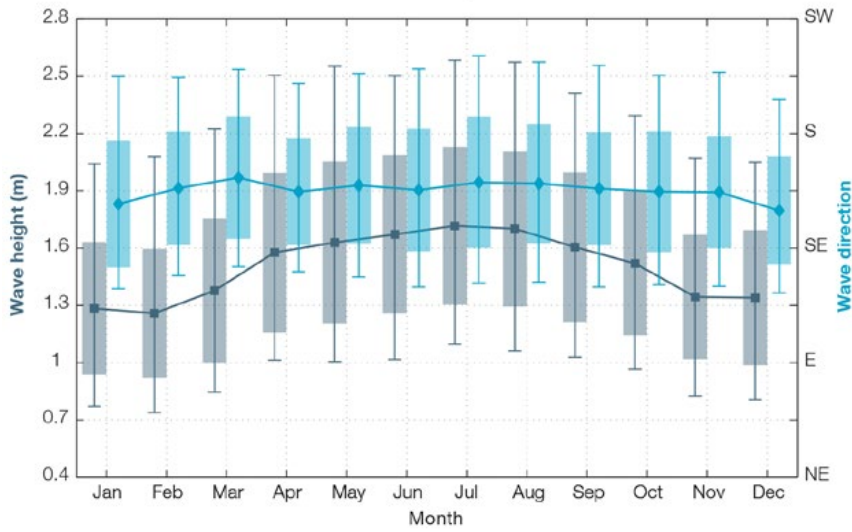


Figure 5.1: Mean annual cycle of wave height (grey) and mean wave direction (blue) at Suva in hindcast data (1979–2009). To give an indication of interannual variability of the monthly means of the hindcast data, shaded boxes show 1 standard deviation around the monthly means, and error bars show the 5–95% range. The direction from which the waves are travelling is shown (not the direction towards which they are travelling).

Mean annual cycle of wave height and mean wave direction (hindcast)
Nadi, Fiji

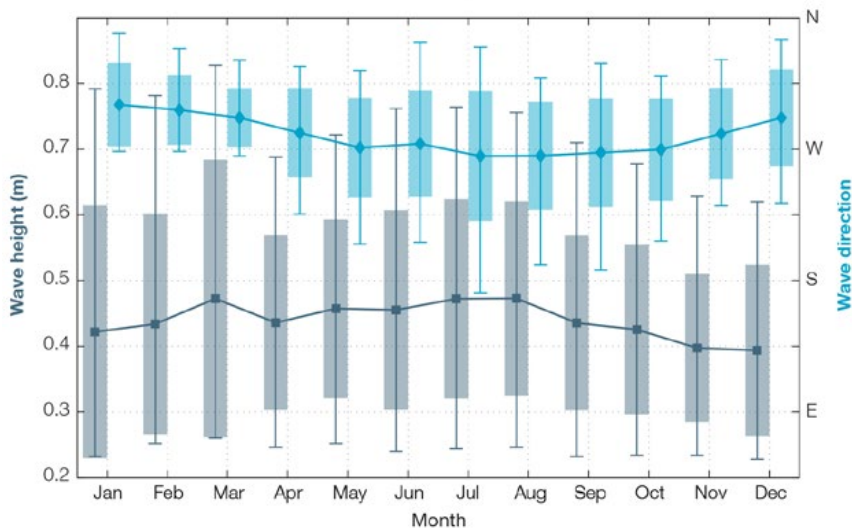


Figure 5.2: Mean annual cycle of wave height (grey) and mean wave direction (blue) at Nadi in hindcast data (1979–2009). To give an indication of interannual variability of the monthly means of the hindcast data, shaded boxes show 1 standard deviation around the monthly means, and error bars show the 5–95% range. The direction from which the waves are travelling is shown (not the direction towards which they are travelling).

5.4 Observed Trends

5.4.1 Air Temperature

Annual and Half-year Mean Air Temperature

Maximum and minimum temperatures have been increasing at both Suva and Nadi Airport since 1942 (Figure 5.3, Figure 5.4 and Table 5.2). All of these temperature trends are statistically significant at the 5% level, with the exception of the Nadi Airport maximum temperature trends in November–April. Minimum temperature trends are stronger than maximum temperature trends.

Extreme Daily Air Temperature

Trends in night-time extreme daily temperatures were found to be stronger than day-time extreme temperatures (Table 5.3; Figure 5.5). At both Suva and Nadi Airport there have been statistically significant decreases in annual Cool Days and Cool Nights and significant increases in the annual Warm Nights. Warm Days have increased at Suva but not at Nadi Airport where the trend is not significant.

The positive trends in air temperatures at Laucala Bay, Suva are larger than expected for this part of the Pacific. This appears to be due to gradual changes in the environment around the observation site since 1942. Large trees and buildings surround the observation site which previously appeared (from photographs) to be more exposed to the cool south-easterly trade-winds. A large area of mangrove to the west has also been filled in and built on in recent years.

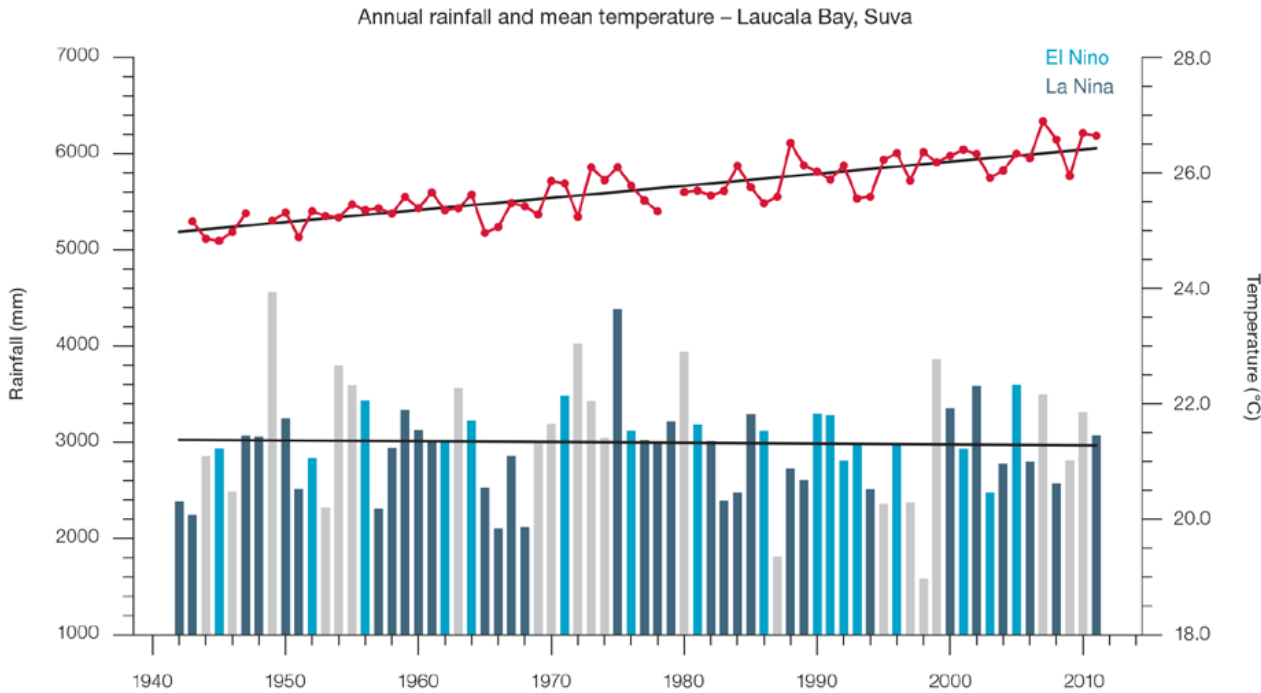


Figure 5.3: Observed time series of annual average values of mean air temperature (red dots and line) and total rainfall (bars) at Suva. Light blue, dark blue and grey bars denote El Niño, La Niña and neutral years respectively. Solid black trend lines indicate a least squares fit.

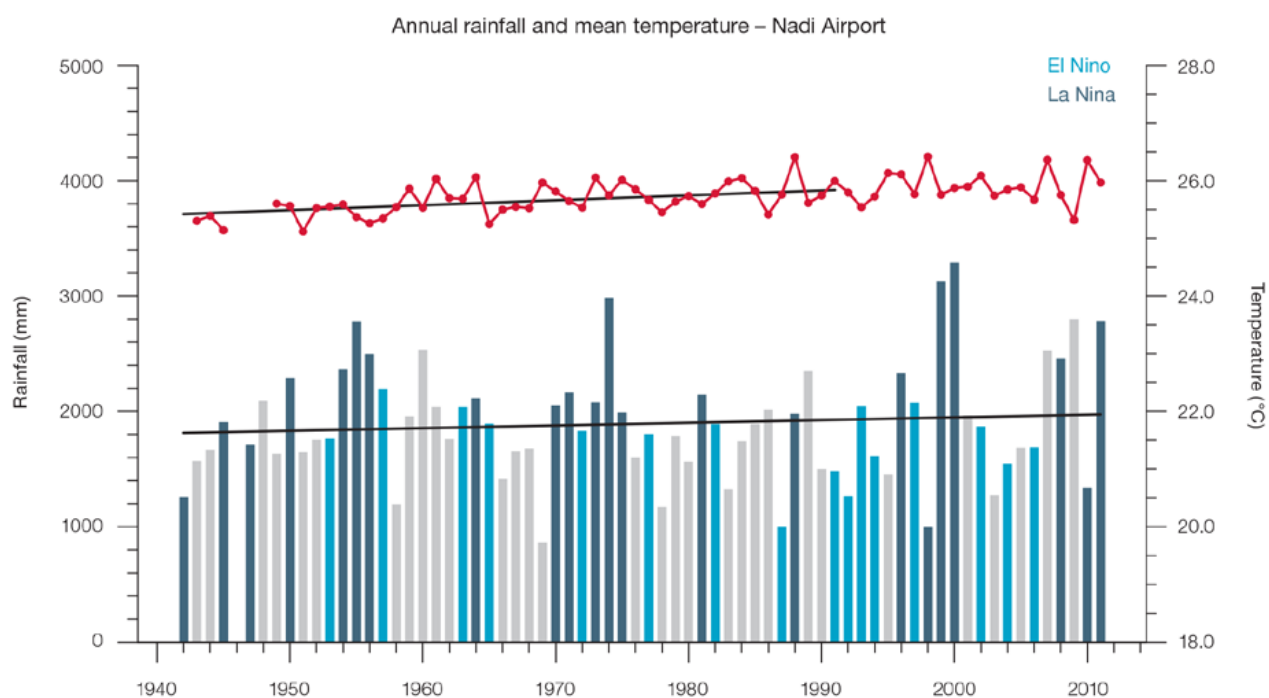


Figure 5.4: Observed time series of annual average values of mean air temperature (red dots and line) and total rainfall (bars) at Nadi Airport. Light blue, dark blue and grey bars denote El Niño, La Niña and neutral years respectively. Solid black trend lines indicate a least squares fit.

Table 5.2: Annual and half-year trends in air temperature (Tmax, Tmin, Tmean) and rainfall at Suva (top) and Nadi Airport (bottom) for the period 1942–2011. The 95% confidence intervals are shown in parentheses. Values for trends significant at the 5% level are shown in boldface.

Suva	Tmax (°C/10yrs)	Tmin (°C/10yrs)	Tmean (°C/10yrs)	Total Rain (mm/10yrs)
Annual	+0.15 (+0.10, +0.20)	+0.26 (+0.22, +0.30)	+0.21 (+0.17, +0.25)	-9.4 (-81.5, +55.7)
Nov-Apr	+0.17 (+0.09, +0.25)	+0.28 (+0.21, +0.34)	+0.22 (+0.16, +0.28)	-38.7 (-93.0, +15.8)
May-Oct	+0.16 (+0.12, +0.20)	+0.28 (+0.10, +0.46)	+0.24 (+0.08, +0.36)	+15.2 (-28.7, +60.6)

Nadi Airport	Tmax (°C /10yrs)	Tmin (°C/10yrs)	Tmean (°C/10yrs)	Total Rain (mm/10yrs)
Annual	+0.04 (+0.01, +0.08)	+0.13 (+0.09, +0.18)	+0.08 (+0.04, +0.12)	-3.3 (-79.5, +76.8)
Nov-Apr	+0.01 (-0.04, +0.06)	+0.13 (+0.08, +0.17)	+0.08 (+0.04, +0.11)	+14.0 (-50.8, +76.3)
May-Oct	+0.06 (+0.01, +0.12)	+0.14 (+0.06, +0.21)	+0.10 (+0.03, +0.16)	-6.2 (-25.1, +17.2)

Table 5.3: Annual trends in air temperature and rainfall extremes at Suva (left) and Nadi Airport (right) for the period 1942–2011. The 95% confidence intervals are shown in parentheses. Values for trends significant at the 5% level are shown in **boldface**.

	Suva	Nadi Airport
TEMPERATURE	1942–2011	
Warm Days (days/decade)	4.19 (+1.32, +7.58)	1.46 (-0.30, +3.15)
Warm Nights (days/decade)	7.87 (+5.83, +10.62)	5.97 (+2.88, +9.30)
Cool Days (days/decade)	-4.18 (-6.76, -1.60)	-3.10 (-5.01, -1.37)
Cool Nights (days/decade)	-11.81 (-13.51, -10.08)	-6.01 (-9.43, -3.14)
RAINFALL		
Rain Days \geq 1 mm (days/decade)	1.1 (-2.05, +3.82)	-1.45 (-5.13, +2.36)
Very Wet Day rainfall (mm/decade)	-16.02 (-65.20, +31.87)	7.17 (-25.63, +40.12)
Consecutive Dry Days (days/decade)	-0.36 (-0.78, +0.05)	0.31 (-1.58, +2.24)
Max 1-day rainfall (mm/decade)	2.33 (-3.23, +7.36)	-2.91 (-10.19, +3.83)

Warm Days: Number of days with maximum temperature greater than the 90th percentile for the base period 1971–2000

Warm Nights: Number of days with minimum temperature greater than the 90th percentile for the base period 1971–2000

Cool Days: Number of days with maximum temperature less than the 10th percentile for the base period 1971–2000

Cool Nights: Number of days with minimum temperature less than the 10th percentile for the base period 1971–2000

Rain Days \geq 1 mm: Annual count of days where rainfall is greater or equal to 1 mm (0.039 inches)

Very Wet Day rainfall: Amount of rain in a year where daily rainfall is greater than the 95th percentile for the reference period 1971–2000

Consecutive Dry Days: Maximum number of consecutive days in a year with rainfall less than 1 mm (0.039 inches)

Max 1-day rainfall: Annual maximum 1-day rainfall

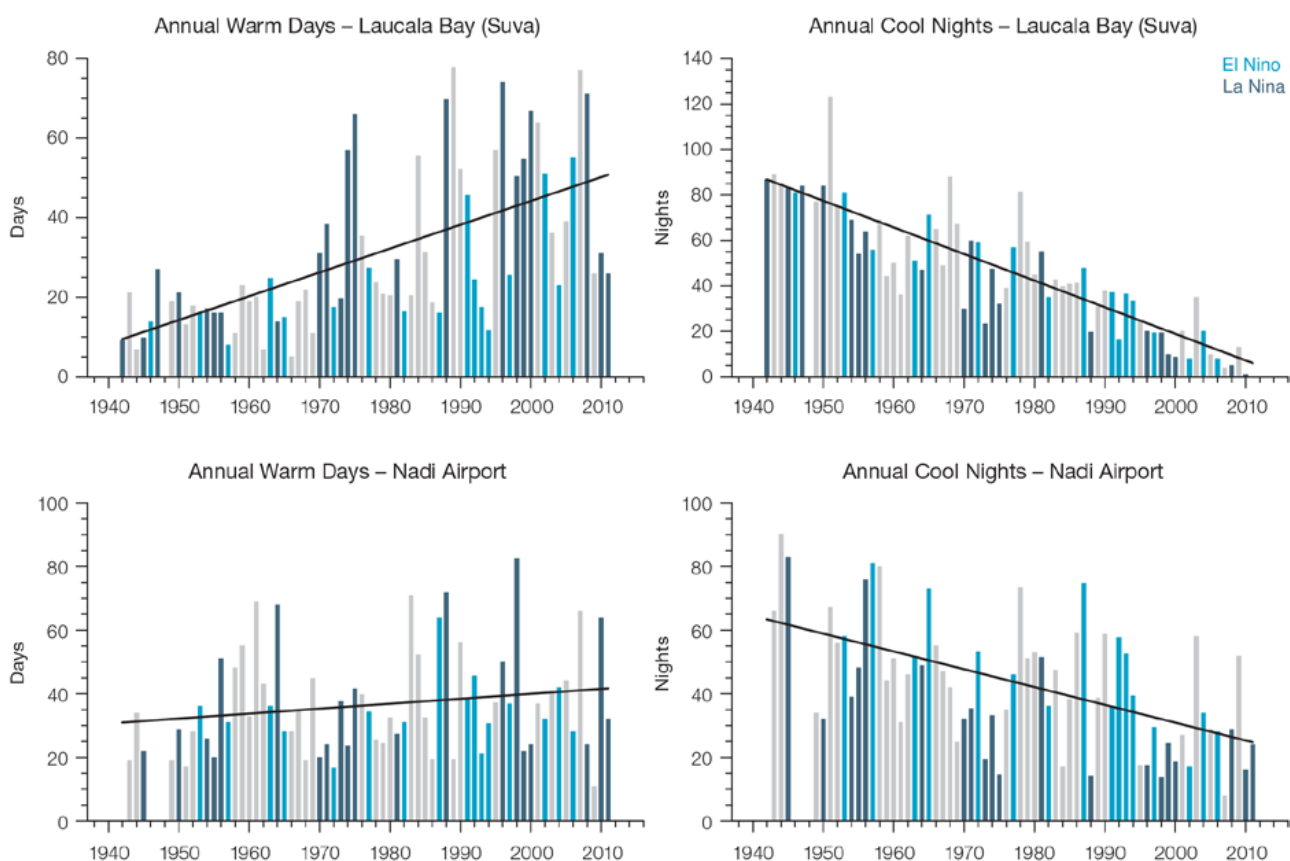


Figure 5.5: Observed time series of annual total number of Warm Days at Suva (top left panel) and Nadi Airport (bottom left panel), and annual Warm Nights at Suva (top right panel) and Nadi Airport (bottom right panel). Solid black line indicates least squares fit.

5.4.2 Rainfall

Annual and Half-year Total Rainfall

Notable interannual variability associated with the ENSO is evident in the observed rainfall records for Nadi Airport (Figure 5.3) and Suva (Figure 5.4) since 1942. Trends in annual and half-year rainfall presented in Table 5.2, Figure 5.3 and Figure 5.4 are not statistically significant at the 5% level. In other words, annual and half-yearly rainfall trends show little change at Suva and Nadi Airport.

Daily Rainfall

Daily rainfall trends for Suva and Nadi Airport are presented in Table 5.3. Due to large year-to-year variability, none of these trends are statistically significant. Figure 5.6 shows insignificant trends in the annual number of Rain Days ≥ 1 mm and Consecutive Dry Days at Suva and Nadi Airport.

5.4.3 Tropical Cyclones

When tropical cyclones affect Fiji they tend to do so between November and April. Tropical cyclones also occasionally occur in October and May in El Niño years. The tropical cyclone archive of the Southern Hemisphere indicates that between the 1969/70 and 2010/11 seasons,

117 tropical cyclones crossed the Fiji Exclusive Economic Zone (EEZ), usually approaching Fiji from the north-west. This represents an average of 28 cyclones per decade. Refer to Chapter 1, Section 1.4.2 (Tropical Cyclones) for an explanation of the difference in the number of tropical cyclones occurring in Fiji in this report (Australian Bureau of Meteorology and CSIRO, 2014) compared to Australian Bureau of Meteorology and CSIRO (2011).

Interannual variability in the number of tropical cyclones in the Fiji EEZ is large, ranging from zero in 1994/95 to six in 1979/80 and 1992/93 (Figure 5.7). The differences between tropical cyclone average occurrence in El Niño, La Niña and neutral years are not statistically significant.

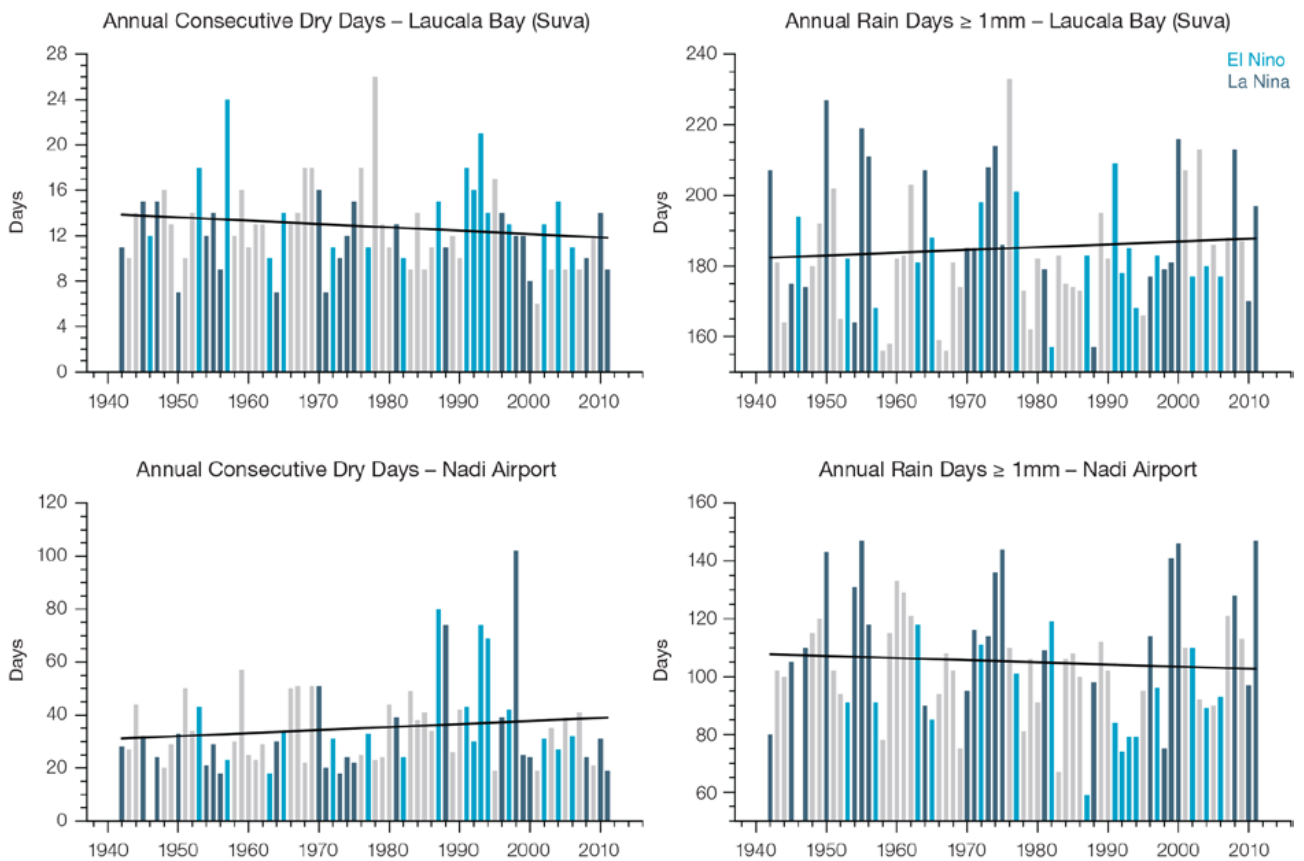


Figure 5.6: Observed time series of annual total number of Consecutive Dry Days at Suva (top left panel) and Nadi Airport (bottom right panel), and annual Rain Days ≥ 1 mm at Suva (top right panel) and Nadi Airport (bottom right panel). Solid black line indicates least squares fit.

Twenty-five of the 78 tropical cyclones (32%) between the 1981/82 and 2010/11 seasons became severe events (Category 3 or stronger) in the Fiji EEZ.

Long term trends in frequency and intensity have not been presented as country scale assessment is not recommended. Some tropical cyclone tracks analysed in this subsection include the tropical depression stage (sustained winds less than or equal to 34 knots) before and/or after tropical cyclone formation.

Additional information on historical tropical cyclones in the Fiji region can be found at www.bom.gov.au/cyclone/history/tracks/index.shtml

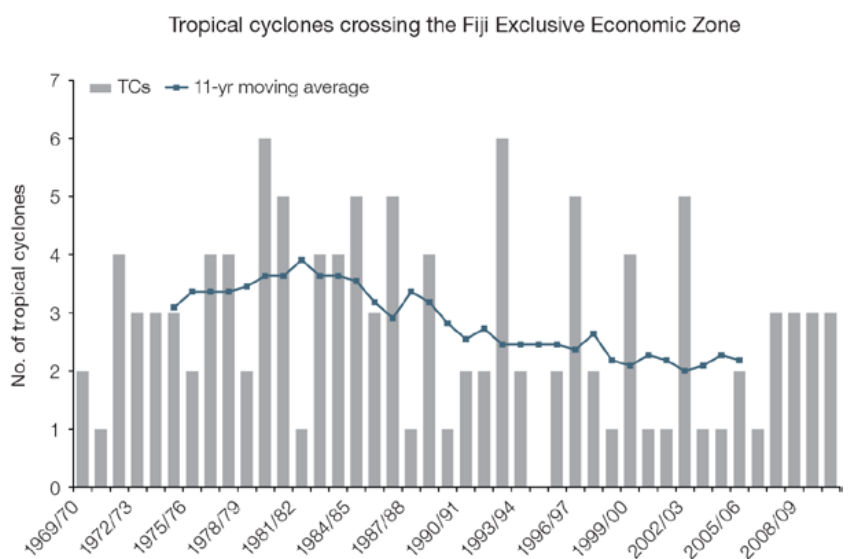


Figure 5.7: Time series of the observed number of tropical cyclones developing within and crossing the Fiji EEZ per season. The 11-year moving average is in blue.

5.5 Climate Projections

The performance of the available Coupled Model Intercomparison Project (Phase 5) (CMIP5) climate models over the Pacific has been rigorously assessed (Brown et al., 2013a, b; Grose et al., 2014; Widlansky et al., 2013). The simulation of the key processes and features for the Fiji region is similar to the previous generation of CMIP3 models, with all the same strengths and many of the same weaknesses. The best-performing CMIP5 models used here have lower biases (differences between the simulated and observed climate data) than the best CMIP3 models, and there are fewer poorly-performing models. For Fiji, the most important model bias is that the rainfall maximum of the SPCZ is too zonally (east-west) oriented. This lowers confidence in the model projections. Out of 27 models assessed, three models were rejected for use in these projections due to biases in the mean climate and in

the simulation of the SPCZ. Climate projections have been derived from up to 24 new GCMs in the CMIP5 database (the exact number is different for each scenario, Appendix A), compared with up to 18 models in the CMIP3 database reported in Australian Bureau of Meteorology and CSIRO (2011).

It is important to realise that the models used give different projections under the same scenario. This means there is not a single projected future for Fiji, but rather a range of possible futures for each emission scenario. This range is described below.

5.5.1 Temperature

Further warming is expected over Fiji (Figure 5.8, Table 5.6). Under all RCPs, the warming is up to 1.0°C by 2030, relative to 1995, but after 2030 there is a growing difference

in warming between each RCP. For example, in Fiji by 2090, a warming of 1.9 to 4.0°C is projected for RCP8.5 (very high emissions) while a warming of 0.3 to 1.1°C is projected for RCP2.6 (very low emissions). This range is broader than that presented in Australian Bureau of Meteorology and CSIRO (2011) because a wider range of emissions scenarios is considered. While relatively warm and cool years and decades will still occur due to natural variability, there is projected to be more warm years and decades on average in a warmer climate. Dynamical downscaling of climate models (Australian Bureau of Meteorology and CSIRO, 2011, Volume 1, Chapter 7) suggests that temperature rises may be about 0.4°C greater over land than over ocean in this area.

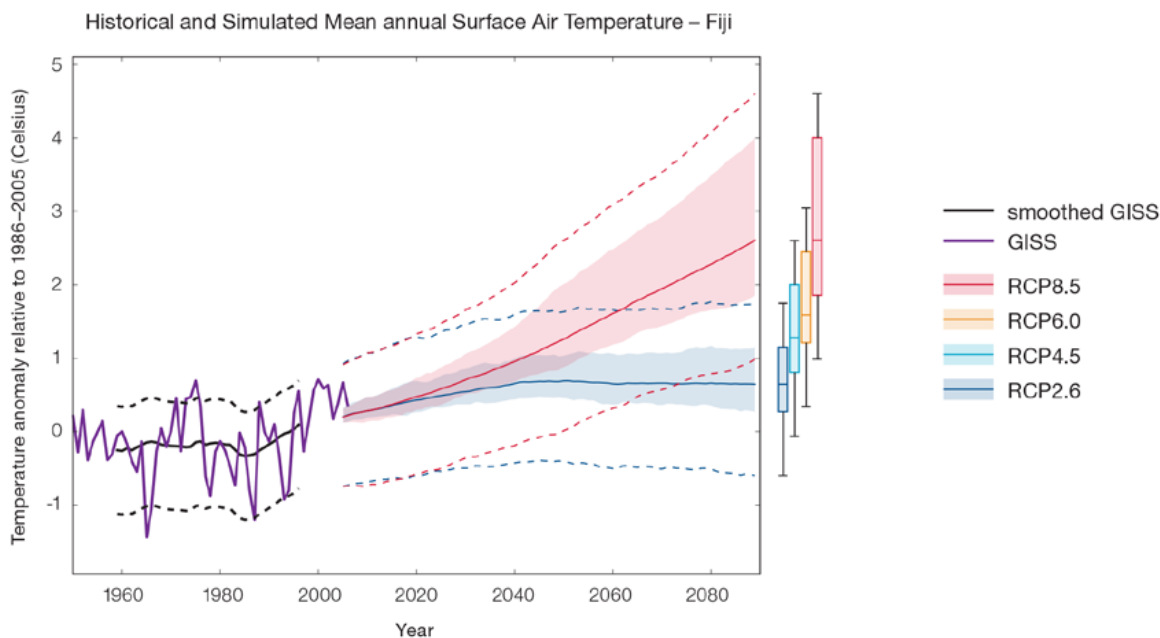


Figure 5.8: Historical and simulated surface air temperature time series for the region surrounding Fiji. The graph shows the anomaly (from the base period 1986–2005) in surface air temperature from observations (the GISS dataset, in purple), and for the CMIP5 models under the very high (RCP8.5, in red) and very low (RCP2.6, in blue) emissions scenarios. The solid red and blue lines show the smoothed (20-year running average) multi-model mean anomaly in surface air temperature, while shading represents the spread of model values (5–95th percentile). The dashed lines show the 5–95th percentile of the observed interannual variability for the observed period (in black) and added to the projections as a visual guide (in red and blue). This indicates that future surface air temperature could be above or below the projected long-term averages due to interannual variability. The ranges of projections for a 20-year period centred on 2090 are shown by the bars on the right for RCP8.5, 6.0, 4.5 and 2.6.

There is *very high confidence* that temperatures will rise because:

- It is known from theory and observations that an increase in greenhouse gases will lead to a warming of the atmosphere; and
- Climate models agree that the long-term average temperature will rise.

There is *medium confidence* in the model average temperature change shown in Table 5.6 because:

- The new models do not simulate the temperature change of the recent past in Fiji as well as in other places; and
- There are biases in the simulation of sea-surface temperatures in the region of Fiji, and associated biases in the simulation of the South Pacific Convergence Zone, which affect projections of both temperature and rainfall.

5.5.2 Rainfall

The CMIP5 models show a range of projected annual rainfall change from an increase to a decrease, and the model average indicates little change. The range is greater in the highest emissions scenarios (Figure 5.9, Table 5.6). Similar to the CMIP3 results, there is greater model agreement for a slight increase in November–April rainfall in the Fiji region. There is a range of projections for May–October rainfall with the model average indicating little change. This is different from Australian Bureau of Meteorology and CSIRO (2011), which reported a slight decrease projected in May–October rainfall.

The year-to-year rainfall variability over Fiji is generally larger than the projected change, except for the models with the largest projected

change in the highest emission scenario by 2090. The effect of climate change on average rainfall may not be obvious in the short or medium term due to natural variability. Dynamical downscaling of climate models suggests that rainfall changes may be different in the east (windward) side of the island compared to the west (leeward) side of the island. In the November–April season CCAM indicates for a group of three models that project a mean rainfall increase over the entire region, rainfall may increase more than the regional average on the west, but increase less or even decrease in the eastern half of the two main Fijian islands. CCAM indicates any east-west pattern to be weak in the May–October season.

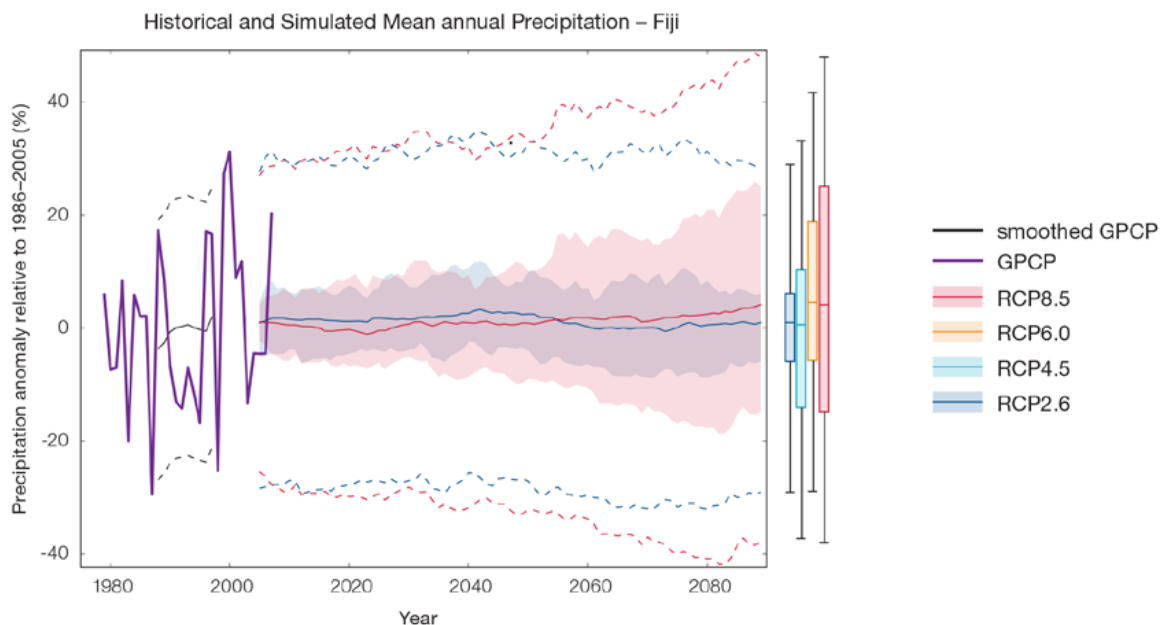


Figure 5.9: Historical and simulated annual average rainfall time series for the region surrounding Fiji. The graph shows the anomaly (from the base period 1986–2005) in rainfall from observations (the GPCP dataset, in purple), and for the CMIP5 models under the very high (RCP8.5, in red) and very low (RCP2.6, in blue) emissions scenarios. The solid red and blue lines show the smoothed (20-year running average) multi-model mean anomaly in rainfall, while shading represents the spread of model values (5–95th percentile). The dashed lines show the 5–95th percentile of the observed interannual variability for the observed period (in black) and added to the projections as a visual guide (in red and blue). This indicates that future rainfall could be above or below the projected long-term averages due to interannual variability. The ranges of projections for a 20-year period centred on 2090 are shown by the bars on the right for RCP8.5, 6.0, 4.5 and 2.6.

There is no agreement on the direction of annual average rainfall change in the models, and many models project little change in annual rainfall. This lowers the confidence that we can determine the most likely direction of change in annual rainfall. The 5–95th percentile range of projected values from CMIP5 climate models for RCP8.5 (very high emissions) is -5 to +9% by 2030 and -15 to +25% by 2090.

There is *low confidence* that the average annual rainfall will not change, because:

- The finding of little change to average annual rainfall is the average of a large model spread from a projected rainfall increase to a rainfall decrease, including many models that project little change;
- Changes in SPCZ rainfall are uncertain. The majority of CMIP5 models simulate increased rainfall in the western part of the SPCZ (Brown et al., 2013a) and decreased rainfall in the eastern part of the SPCZ, however rainfall changes are sensitive to sea-surface temperature gradients, which are not well simulated in many models (Widlansky et al., 2013). See Box 1 in Chapter 1 for more details; and
- Dynamical downscaling also does not indicate a consistent direction of change (some simulations show increased rainfall, others show decreased rainfall).

There is *low confidence* in the model average rainfall change shown in Table 5.6 because:

- There is a spread in model rainfall projections, which range from a projected rainfall increase to a rainfall decrease;
- The complex set of processes involved in tropical rainfall is challenging to simulate in models. This means that the confidence in the projection of rainfall is generally lower than for other variables such as temperature;

- There is a different magnitude of change in SPCZ rainfall projected by models that have reduced sea-surface temperature biases (Australian Bureau of Meteorology and CSIRO, 2011, Chapter 7 (downscaling); Widlansky et al., 2012) compared to the CMIP5 models; and
- The future behaviour of the El Niño–Southern Oscillation is unclear, and the El Niño–Southern Oscillation strongly influences year-to-year rainfall variability.

5.5.3 Extremes

Extreme Temperature

The temperature on extremely hot days is projected to increase by about the same amount as average temperature. This conclusion is based on analysis of daily temperature data from a subset of CMIP5 models (Chapter 1). The frequency of extremely hot days is also expected to increase.

The temperature of the 1-in-20-year hot day is projected to increase by approximately 0.6°C by 2030 under the RCP2.6 (very low) scenario and by 0.8°C under the RCP8.5 (very high) scenario. By 2090 the projected increase is 0.7°C for RCP2.6 (very low) and 3°C for RCP8.5 (very high).

There is *very high confidence* that the temperature of extremely hot days and the temperature of extremely cool days will increase, because:

- A change in the range of temperatures, including the extremes, is physically consistent with rising greenhouse gas concentrations;
- This is consistent with observed changes in extreme temperatures around the world over recent decades; and
- All the CMIP5 models agree on an increase in the frequency and intensity of extremely hot days and a decrease in the frequency and intensity of cool days.

There is *low confidence* in the magnitude of projected change in extreme temperature because models generally underestimate the current intensity and frequency of extreme events, especially in this area, due to the ‘cold-tongue bias’ (Chapter 1). Changes to the particular driver of extreme temperatures affect whether the change to extremes is more or less than the change in the average temperature, and the changes to the drivers of extreme temperatures in Fiji are currently unclear. Also, while all models project the same direction of change there is a wide range in the projected magnitude of change among the models.

Extreme Rainfall

The frequency and intensity of extreme rainfall events are projected to increase. This conclusion is based on analysis of daily rainfall data from a subset of CMIP5 models using a similar method to that in Australian Bureau of Meteorology and CSIRO (2011) with some improvements (Chapter 1), so the results are slightly different to those in Australian Bureau of Meteorology and CSIRO (2011). The current 1-in-20-year daily rainfall amount is projected to increase by approximately 5 mm by 2030 for RCP2.6 and by 7 mm by 2030 for RCP8.5 (very high emissions). By 2090, it is projected to increase by approximately 6 mm for RCP2.6 and by 36 mm for RCP8.5 (very high emissions). The majority of models project the current 1-in-20-year daily rainfall event will become, on average, a 1-in-9-year event for RCP2.6 and a 1-in-4-year event for RCP8.5 (very high emissions) by 2090. These results are different to those found in Australian Bureau of Meteorology and CSIRO (2011) because of different methods used (Chapter 1).

There is *high confidence* that the frequency and intensity of extreme rainfall events will increase because:

- A warmer atmosphere can hold more moisture, so there is greater potential for extreme rainfall (IPCC, 2012);
- Increases in extreme rainfall in the Pacific are projected in all available climate models; and
- An increase in extreme rainfall events within the SPCZ region was found by an in-depth study of extreme rainfall events in the SPCZ (Cai et al., 2012).

There is *low confidence* in the magnitude of projected change in extreme rainfall because:

- Models generally underestimate the current intensity of local extreme events, especially in this area due to the 'cold-tongue bias' (Chapter 1);
- Changes in extreme rainfall projected by models may be underestimated because models seem to underestimate the observed increase in heavy rainfall with warming (Min et al., 2011);
- GCMs have a coarse spatial resolution, so they do not adequately capture some of the

processes involved in extreme rainfall events; and

- The Conformal Cubic Atmospheric Model (CCAM) downscaling model has finer spatial resolution and the CCAM results presented in Australian Bureau of Meteorology and CSIRO (2011) indicates a smaller increase in the number of extreme rainfall days, and there is no clear reason to accept one set of models over another.

Drought

Drought projections (defined in Chapter 1) are described in terms of changes in proportion of time in drought, frequency and duration by 2090 for very low and very high emissions (RCP2.6 and 8.5).

For Fiji the overall proportion of time spent in drought is expected to decrease slightly under all scenarios. Under RCP8.5 the frequency of drought in all categories is projected to decrease and the duration of events is projected to stay approximately the same (Figure 5.10). Under RCP2.6 (very low emissions) the frequency of mild and moderate drought events is expected to decrease slightly

while the frequency of severe and extreme events is projected to stay approximately the same. The duration of events in all drought categories is projected to stay approximately the same under RCP2.6 (very low emissions). These results are different to those found in Australian Bureau of Meteorology and CSIRO (2011), which reported little change in drought was likely for Fiji.

There is *low confidence* in this direction of change because:

- There is only *low confidence* in the direction of mean rainfall change;
- These drought projections are based upon a subset of models; and
- Like the CMIP3 models, the majority of the CMIP5 models agree on this direction of change.

There is *low confidence* in the projections of drought frequency and duration because there is *low confidence* in the magnitude of rainfall projections, and no consensus about projected changes in the ENSO, which directly influence the projection of drought.

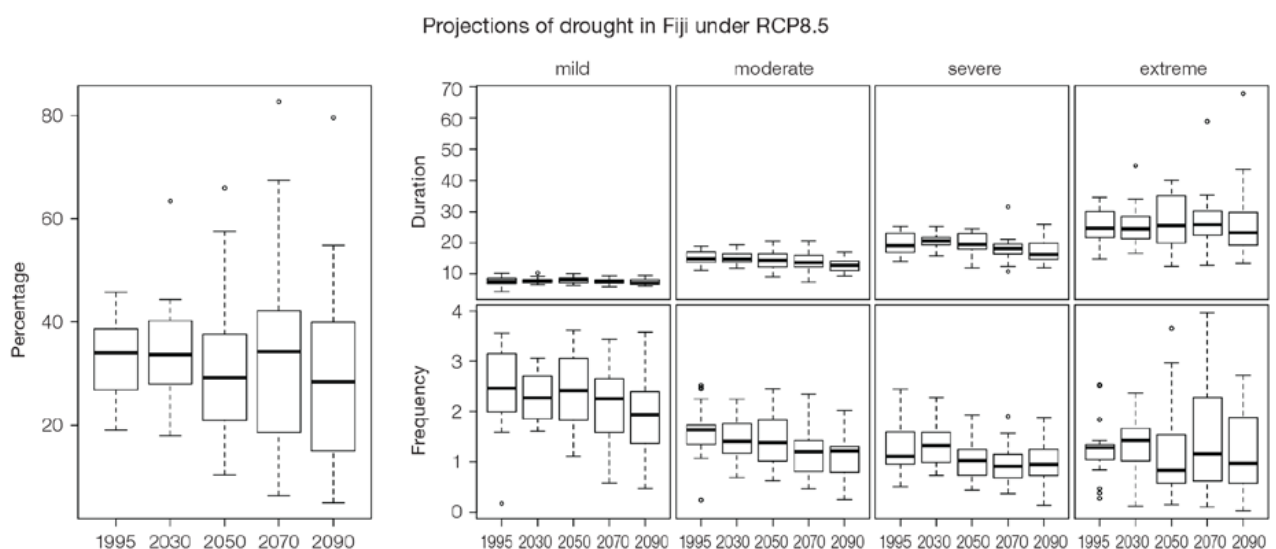


Figure 5.10: Box-plots showing percent of time in moderate, severe or extreme drought (left hand side), and average drought duration and frequency for the different categories of drought (mild, moderate, severe and extreme) for Fiji. These are shown for 20-year periods centred on 1995, 2030, 2050, 2070 and 2090 for the RCP8.5 (very high emissions) scenario. The thick dark lines show the median of all models, the box shows the interquartile (25–75%) range, the dashed lines show 1.5 times the interquartile range and circles show outlier results.

Tropical Cyclones

Global Picture

There is a growing level of consistency between models that on a global basis the frequency of tropical cyclones is likely to decrease by the end of the 21st century. The magnitude of the decrease varies from 6%–35% depending on the modelling study. There is also a general agreement between models that there will be an increase in the mean maximum wind speed of cyclones by between 2% and 11% globally, and an increase in rainfall rates of the order of 20% within 100 km of the cyclone centre (Knutson et al., 2010). Thus, the scientific community has a *medium* level of confidence in these global projections.

Fiji

In Fiji, the projection is for a decrease in cyclone genesis (formation) frequency for the south-east basin (see Figure 5.11 and Table 5.4). The confidence level for this projection is high. The GCMs show consistent results across models for changes in cyclone frequency for the south-east basin, using the direct detection methodologies (OWZ or CDD) described in Chapter 1. Approximately 80% of the projected changes, based on these methods, vary between a 5% decrease to a 50% decrease in genesis frequency with half projecting a decrease between 20 and 40%. The empirical techniques assess changes in the main atmospheric ingredients known to be necessary for cyclone formation. Projections based upon these techniques suggest the conditions for cyclone formation will become less favourable in this region with about half of projected changes indicating decreases between 10 and 40% in genesis frequency. These projections are consistent with those of Australian Bureau of Meteorology and CSIRO (2011).

Table 5.4: Projected percentage change in cyclone frequency in the south-east basin (0–40°S; 170°E–130°W) for 22 CMIP5 climate models, based on five methods, for 2080–2099 relative to 1980–1999 for RCP8.5 (very high emissions). The 22 CMIP5 climate models were selected based upon the availability of data or on their ability to reproduce a current-climate tropical cyclone climatology (See Section 1.5.3 – Detailed Projection Methods, Tropical Cyclones). Blue numbers indicate projected decreases in tropical cyclone frequency, red numbers an increase. MMM is the multi-model mean change. N increase is the proportion of models (for the individual projection method) projecting an increase in cyclone formation.

Model	GPI change	GPI-M change	Tippett	CDD	OWZ
access10	5	-22	-54	-23	
access13	-26	-26	-36	-10	
bccscm11	-3	-1	-28		-5
canesm2	-7	-13	-49	-6	
ccsm4				-78	-5
cnrm_cm5	-4	-5	-26	8	7
csiro_mk36	-16	-13	-33	-26	-27
fgoals_g2	6	-8	-40		
fgoals_s2	-15	-20	-48		
gfdl_esm2m				-48	-36
gfdl_cm3	-1	-5	-25		-11
gfdl_esm2g				-18	-36
gisse2r	17	16	-6		
hadgem2_es	-8	-11	-51		
inm	-3	-3	-30		
ipslcm5alr	-13	-19	-43		
ipslcm5blr				7	
miroc5				-43	-22
miroc5m	-40	-38	46		
mpim	-26	-19	-41		
mri_cgcm3	-8	-10	-28		
noresm1m	-36	-40	-59	-80	
MMM	-11	-14	-32	-29	-17
N increase	0.2	0.1	0.1	0.2	0.125

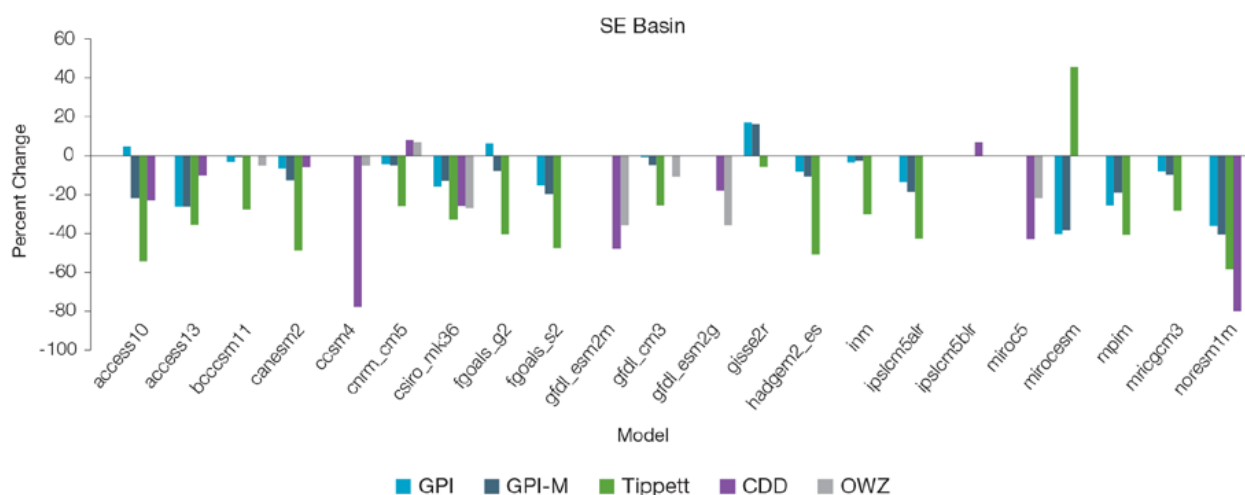


Figure 5.11: Projected percentage change in cyclone frequency in the south-east basin (data from Table 5.4).

5.5.4 Coral Reefs and Ocean Acidification

As atmospheric CO₂ concentrations continue to rise, oceans will warm and continue to acidify. These changes will impact the health and viability of marine ecosystems, including coral reefs that provide many key ecosystem services (*high confidence*). These impacts are also likely to be compounded by other stressors such as storm damage, fishing pressure and other human impacts.

The projections for future ocean acidification and coral bleaching use three RCPs (2.6, 4.5, and 8.5).

Ocean Acidification

Ocean acidification is expressed in terms of aragonite saturation state (Chapter 1). In the Fiji region, the aragonite saturation state has declined from about 4.5 in the late 18th century to an observed value of about 3.9±0.1 by 2000 (Kuchinke et al., 2014). All models show that the aragonite saturation state, a proxy for coral reef growth rate, will continue to decrease as atmospheric CO₂ concentrations increase (*very high confidence*). Projections from CMIP5 models indicate that under RCPs 8.5 (very high emissions) and 4.5 (low emissions) the median aragonite saturation state will transition to marginal conditions (3.5) around 2030. In RCP8.5 (very high emissions) the aragonite saturation state continues to strongly decline thereafter to

values where coral reefs have not historically been found (< 3.0). Under RCP4.5 (low emissions) the aragonite saturation plateaus around 3.2 i.e. marginal conditions for healthy coral reefs. While under RCP2.6 (very low emissions) the median aragonite saturation state never falls below 3.5, and increases slightly toward the end of the century (Figure 5.12) suggesting that the conditions remains adequate for healthy corals reefs. There is *medium confidence* in this range and distribution of possible futures because the projections are based on climate models that do not resolve the reef scale that can play a role in modulating large-scale changes. The impacts of ocean acidification are also likely to affect the entire marine ecosystem impacting the key ecosystem services provided by reefs.

Projected decreases in aragonite saturation state for Fiji

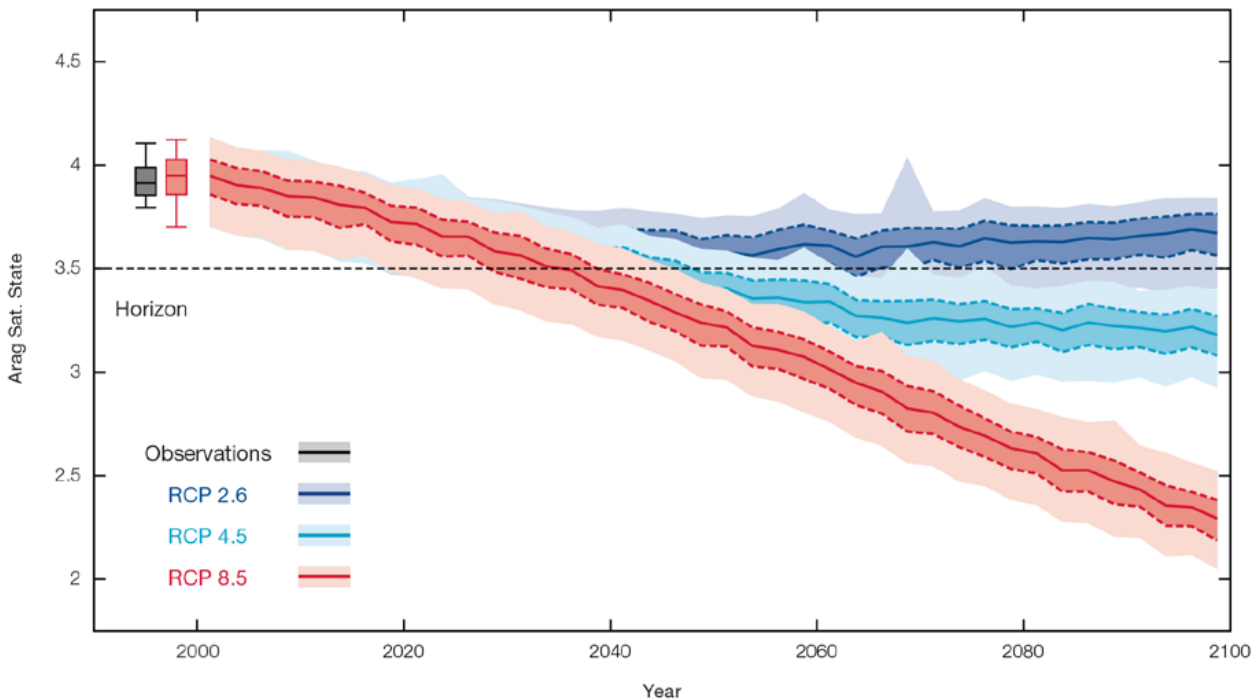


Figure 5.12: Projected decreases in aragonite saturation state for Fiji from CMIP5 models under RCP2.6, 4.5 and 8.5. Shown are the median values (solid lines), the interquartile range (dashed lines), and 5% and 95% percentiles (light shading). The horizontal line represents the transition to marginal conditions for coral reef health (from Guinotte et al., 2003).

Coral Bleaching Risk

As the ocean warms, the risk of coral bleaching increases (*very high confidence*). There is *medium confidence* in the projected rate of change for Fiji because there is *medium confidence* in the rate of change of sea-surface temperature (SST), and the changes at the reef scale (which can play a role in modulating large-scale changes) are not adequately resolved. Importantly, the coral bleaching risk calculation does not account the impact of other potential stressors (Chapter 1).

The changes in the frequency (or recurrence) and duration of severe bleaching risk are quantified for different projected SST changes (Table 5.5). Overall there is a decrease in the time between two periods of elevated risk and an increase in the duration of the elevated risk. For example, under a long-term mean increase of 1°C (relative to 1982–1999 period), the average period of severe

bleaching risk (referred to as a risk event) will last 7.9 weeks (with a minimum duration of 2.6 weeks and a maximum duration of 3.3 months) and the average time between two risks will be 3.5 years (with the minimum

recurrence of 8.3 months and a maximum recurrence of 10.2 years). If severe bleaching events occur more often than once every five years, the long-term viability of coral reef ecosystems becomes threatened.

Table 5.5: Projected changes in severe coral bleaching risk for the Fiji EEZ for increases in SST relative to 1982–1999.

Temperature change ¹	Recurrence interval ²	Duration of the risk event ³
Change in observed mean	0	0
+0.25°C	29.3 years (29.2 years – 29.3 years)	4.3 weeks (4.2 weeks – 4.3 weeks)
+0.5°C	23.6 years (22.7 years – 24.5 years)	5.3 weeks (4.9 weeks – 5.8 weeks)
+0.75°C	13.1 years (7.9 years – 18.7 years)	6.4 weeks (4.0 weeks – 8.7 weeks)
+1°C	3.5 years (8.3 months – 10.2 years)	7.9 weeks (2.6 weeks – 3.3 months)
+1.5°C	11.7 months (6.4 months – 2.0 years)	2.9 months (3.5 weeks – 5.0 months)
+2°C	8.1 months (5.7 months – 1.4 years)	4.6 months (1.7 months – 6.4 months)

¹ This refers to projected SST anomalies above the mean for 1982–1999.

² Recurrence is the mean time between severe coral bleaching risk events. Range (min – max) shown in brackets.

³ Duration refers to the period of time where coral are exposed to the risk of severe bleaching. Range (min – max) shown in brackets.

5.5.5 Sea Level

Mean sea level is projected to continue to rise over the course of the 21st century. There is *very high confidence* in the direction of change. The CMIP5 models simulate a rise of between approximately 8–18 cm by 2030 (very similar values for different RCPs), with increases of 41–88 cm by 2090 under the RCP8.5 (Figure 5.13 and Table 5.6). There is *medium confidence* in the range mainly because there is still uncertainty associated with projections of the Antarctic ice sheet contribution. Interannual variability of sea level will lead to periods of lower and higher regional sea levels. In the past, this interannual variability has been about 18 cm (5–95% range, after removal of the seasonal signal, see dashed lines in Figure 5.13 (a) and it is likely that a similar range will continue through the 21st century.

5.5.6 Wind-driven Waves

During December–March in Fiji, projected changes in wave properties include a decrease in mean wave height of approximately 8 cm (significant only under the high emission RCP8.5, very high emissions, scenario in 2090), accompanied by a small decrease in wave period and a possible clockwise rotation in February (more waves from the south-west) (*low confidence*) (Table 5.7). These features are characteristic of a decrease in strength of the south-easterly trade winds.

In June–September, there are no statistically significant projected changes in wave properties (*low confidence*) (Table 5.7). Non-significant changes include a suggested increase in wave height (Figure 5.14), with a possible increase in period in September. A projected decrease in the larger waves is suggested (*low confidence*).

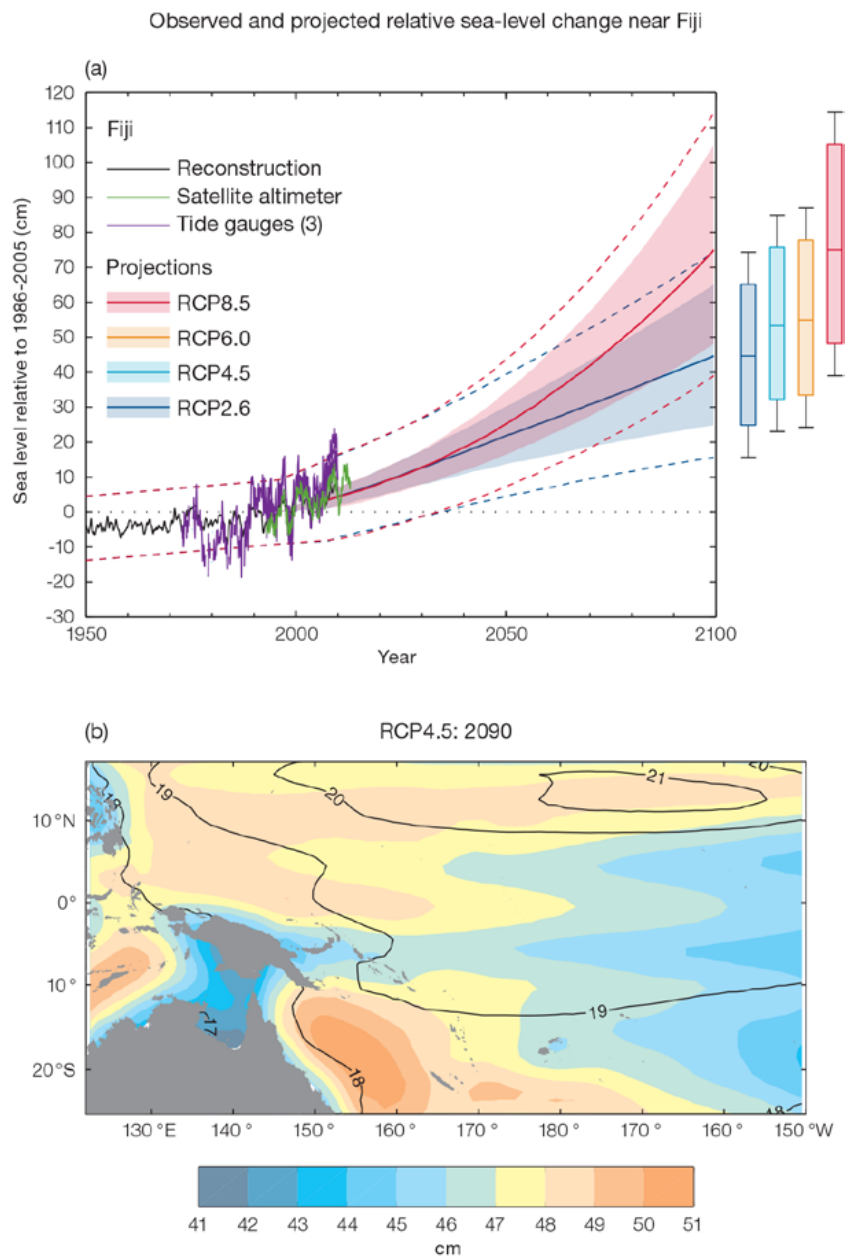


Figure 5.13: (a) The observed tide-gauge records of relative sea-level (since the late 1970s) are indicated in purple, and the satellite record (since 1993) in green. The gridded (reconstructed) sea level data at Fiji (since 1950) is shown in black. Multi-model mean projections from 1995–2100 are given for the RCP8.5 (red solid line) and RCP2.6 emissions scenarios (blue solid line), with the 5–95% uncertainty range shown by the red and blue shaded regions. The ranges of projections for four emission scenarios (RCPs 2.6, 4.5, 6.0 and 8.5) by 2100 are also shown by the bars on the right. The dashed lines are an estimate of interannual variability in sea level (5–95% uncertainty range about the projections) and indicate that individual monthly averages of sea level can be above or below longer-term averages.

(b) The regional distribution of projected sea level rise under the RCP4.5 emissions scenario for 2081–2100 relative to 1986–2005. Mean projected changes are indicated by the shading, and the estimated uncertainty in the projections is indicated by the contours (in cm).

There is *low confidence* in projected changes in the Fiji wind-wave climate because:

- Projected changes in wave climate are dependent on confidence of projected changes in the El Niño–Southern Oscillation, which is low; and
- The difference between simulated and observed (hindcast) waves can be larger than the projected wave changes, which further reduces our confidence in projections.

5.5.7 Projections Summary

There is *very high confidence* in the direction of long-term change in a number of key climate variables, namely an increase in mean and extremely high temperatures, sea level and ocean acidification. There is *high confidence* that the frequency and intensity of extreme rainfall will increase. However, it is unclear whether average annual rainfall and drought frequency will increase, decrease or stay similar to the current climate.

Tables 5.6 and 5.7 quantify the mean changes and ranges of uncertainty

for a number of variables, years and emissions scenarios. A number of factors are considered in assessing confidence, i.e. the type, amount, quality and consistency of evidence (e.g. mechanistic understanding, theory, data, models, expert judgment) and the degree of agreement, following the IPCC guidelines (Mastrandrea et al., 2010). Confidence ratings in the projected magnitude of mean change are generally lower than those for the direction of change (see paragraph above) because magnitude of change is more difficult to assess. For example, there is *very high confidence* that temperature will increase, but *medium confidence* in the magnitude of mean change.

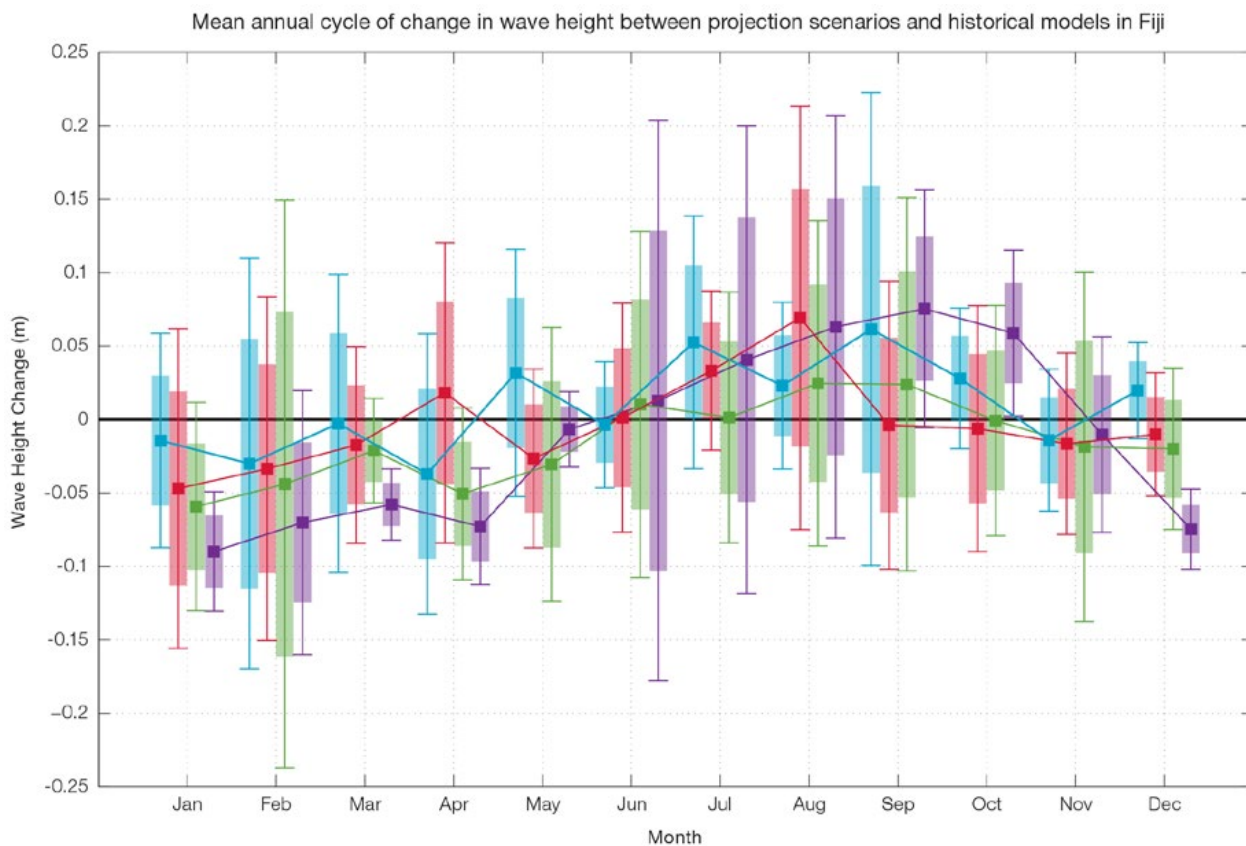


Figure 5.14: Mean annual cycle of change in wave height between projection scenarios and mean of historical models in Fiji. This plot shows a small decrease in wave heights in the wet season months (statistically significant in 2090 RCP8.5, very high emissions), and no change in the drier months. Shaded boxes show 1 standard deviation of models’ means around the ensemble means, and error bars show the 5–95% range inferred from the standard deviation. Colours represent RCP scenarios and time periods: blue 2035 RCP4.5 (low emissions), red 2035 RCP8.5 (very high emissions), green 2090 RCP4.5 (low emissions), purple 2090 RCP8.5 (very high emissions).

Table 5.6: Projected changes in the annual and seasonal mean climate for Fiji under four emissions scenarios; RCP2.6 (very low emissions, in dark blue), RCP4.5 (low emissions, in light blue), RCP6 (medium emissions, in orange) and RCP8.5 (very high emissions, in red). Projected changes are given for four 20-year periods centred on 2030, 2050, 2070 and 2090, relative to a 20-year period centred on 1995. Values represent the multi-model mean change, with the 5–95% range of uncertainty in brackets. Confidence in the magnitude of change is expressed as *high*, *medium* or *low*. Surface air temperatures in the Pacific are closely related to sea-surface temperatures (SST), so the projected changes to air temperature given in this table can be used as a guide to the expected changes to SST. (See also Section 1.5.2). ‘NA’ indicates where data are not available.

Variable	Season	2030	2050	2070	2090	Confidence (magnitude of change)
Surface air temperature (°C)	Annual	0.5 (0.4–0.8)	0.7 (0.5–1)	0.7 (0.4–1.1)	0.6 (0.3–1.1)	<i>Medium</i>
		0.6 (0.3–1)	0.9 (0.6–1.4)	1.1 (0.7–1.8)	1.3 (0.8–2)	
		0.6 (0.4–0.9)	0.9 (0.6–1.3)	1.2 (0.9–1.8)	1.6 (1.2–2.5)	
		0.7 (0.5–1)	1.3 (0.8–2)	1.9 (1.4–2.9)	2.7 (1.9–4)	
Maximum temperature (°C)	1-in-20 year event	0.6 (0.1–0.8)	0.7 (0.2–1.1)	0.7 (0–1)	0.7 (-0.1–1.2)	<i>Medium</i>
		0.6 (0.1–0.9)	0.8 (0.3–1.2)	1.2 (0.5–1.7)	1.3 (0.7–1.9)	
		NA (NA–NA)	NA (NA–NA)	NA (NA–NA)	NA (NA–NA)	
		0.8 (0.1–1.3)	1.4 (0.6–2)	2.2 (1.4–3.1)	2.9 (1.7–4.1)	
Minimum temperature (°C)	1-in-20 year event	0.5 (0.2–0.9)	0.7 (0.2–1.1)	0.7 (0.4–1)	0.6 (0.1–0.8)	<i>Medium</i>
		0.6 (0.3–0.8)	0.9 (0.4–1.3)	1.1 (0.8–1.5)	1.3 (0.9–1.9)	
		NA (NA–NA)	NA (NA–NA)	NA (NA–NA)	NA (NA–NA)	
		0.7 (0.3–1)	1.3 (0.9–1.9)	2.1 (1.6–2.7)	2.9 (2–4.1)	
Total rainfall (%)	Annual	2 (-4–8)	2 (-3–8)	0 (-9–9)	1 (-6–6)	<i>Low</i>
		0 (-7–8)	-1 (-11–7)	2 (-9–14)	1 (-14–10)	
		3 (-3–11)	2 (-8–10)	3 (-7–14)	5 (-6–19)	
		1 (-5–9)	1 (-10–11)	1 (-15–15)	4 (-15–25)	
Total rainfall (%)	Nov-Apr	2 (-3–11)	3 (-4–10)	1 (-7–12)	1 (-5–11)	<i>Low</i>
		1 (-7–10)	0 (-7–10)	4 (-7–20)	2 (-11–13)	
		4 (-4–13)	2 (-9–11)	4 (-8–16)	6 (-7–22)	
		1 (-4–13)	2 (-6–13)	4 (-14–21)	8 (-10–32)	
Total rainfall (%)	May-Oct	2 (-6–9)	2 (-8–11)	0 (-12–9)	1 (-9–11)	<i>Low</i>
		1 (-9–11)	-2 (-12–8)	-1 (-13–11)	0 (-20–10)	
		3 (-9–11)	3 (-6–10)	3 (-11–14)	3 (-7–15)	
		0 (-10–10)	-1 (-14–10)	-2 (-18–12)	-1 (-21–18)	
Aragonite saturation state (Ω_{ar})	Annual	-0.3 (-0.7–0.0)	-0.4 (-0.7–0.1)	-0.4 (-0.7–0.0)	-0.3 (-0.7–0.0)	<i>Medium</i>
		-0.4 (-0.7–0.0)	-0.6 (-0.9–0.3)	-0.7 (-1.0–0.4)	-0.8 (-1.1–0.5)	
		NA (NA–NA)	NA (NA–NA)	NA (NA–NA)	NA (NA–NA)	
		-0.4 (-0.7–0.1)	-0.7 (-1.1–0.4)	-1.1 (-1.4–0.9)	-1.5 (-1.8–1.2)	
Mean sea level (cm)	Annual	13 (8–18)	22 (14–31)	31 (19–44)	41 (24–58)	<i>Medium</i>
		13 (8–18)	23 (14–31)	35 (22–48)	47 (29–67)	
		13 (8–17)	22 (14–31)	34 (22–47)	49 (30–68)	
		13 (8–18)	25 (17–35)	42 (28–58)	64 (41–88)	

Waves Projections Summary

Table 5.7: Projected average changes in wave height, period and direction in Fiji for December–March and June–September for RCP4.5 (low emissions, in blue) and RCP8.5 (very high emissions, in red), for two 20-year periods (2026–2045 and 2081–2100), relative to a 1986–2005 historical period. The values in brackets represent the 5th to 95th percentile range of uncertainty.

Variable	Season	2035	2090	Confidence (range)
Wave height change (m)	December–March	0.0 (-0.2–0.2) -0.0 (-0.2–0.2)	-0.0 (-0.3–0.2) -0.1 (-0.3–0.1)	Low
	June–September	+0.0 (-0.3–0.4) +0.0 (-0.3–0.3)	+0.0 (-0.3–0.4) +0.0 (-0.3–0.4)	Low
Wave period change (s)	December–March	-0.1 (-0.9–0.7) -0.0 (-0.9–0.8)	-0.1 (-1.0–0.8) -0.1 (-1.1–0.9)	Low
	June–September	+0.0 (-0.9–0.9) +0.0 (-0.8–0.9)	+0.1 (-1.0–1.2) +0.1 (-1.1–1.2)	Low
Wave direction change (° clockwise)	December–March	0 (-20–20) 0 (-20–20)	0 (-20–20) 10 (-20–30)	Low
	June–September	0 (-10–10) 0 (-10–10)	0 (-10–10) -0 (-10–10)	Low

Wind-wave variables parameters are calculated for a 20-year period centred on 2035.